Modeling, Identification and Control, Vol. 46, No. 2, 2025, pp. 89–99, ISSN 1890–1328

Control Study of Hydropower System with Francis Turbine in Isolated Operation

Usha Adhikari [1] Pramish Shrestha [1] Bernt Lie [2]

[1] *Department of Electrical and Electronics Engineering, Kathmandu University, Dhulikhel, Nepal.*
E-mail: ushaadhikary25@gmail.com, pramish.shrestha@ku.edu.np

[2] *Department of Electrical Engineering, IT and Cybernetics, University of South-Eastern Norway, Porgrunn, Norway. E-mail:* bernt.lie@usn.no

Abstract

This paper provides a comprehensive examination of controller design for hydropower systems equipped with Francis turbines operating in isolated conditions. By employing a mechanistic modelling approach using differential algebraic equations, the study captures the complex interplay of hydraulic, mechanical, and electrical subsystems, enabling an in-depth analysis of system dynamics under varying load conditions. A two-step approach is adopted, where a PID controller is initially designed for a linearized model and subsequently tested on a nonlinear model, allowing for a systematic evaluation of its performance, in accordance with the Norwegian Transmission System Operator specifications. The controller design process emphasizes achieving critical stability margins, meeting industry standards, and addressing the challenges posed by nonlinear system behaviour. The novelty of this work lies in the use of a recently developed Francis turbine model, its application to a real-world hydropower plant using realistic parameters, and the presentation of the controller design from a control engineering perspective. Directions for future work include exploring optimization-based controller designs, incorporating realistic load profiles, and refining system model to address complex real-world scenarios.

Keywords: Francis turbine, dynamics, nonlinear model of hydropower plant, stability, PID controller

1 Introduction

The growing demand for electricity in modern society, coupled with the need to comply with stricter environmental regulations and the depletion of fossil fuel reserves, is driving a transition toward greater reliance on sustainable and renewable energy sources Vinod et al. (2022). Hydropower remains one of the most reliable and sustainable sources of renewable energy, contributing significantly to global electricity generation. With vast potential for hydropower production, countries such as Nepal and Norway are still facing challenges in optimizing power generation and ensuring grid stability Gunatilake et al. (2020). As electricity demand continues to grow and power grids become more complex, the need for advanced control mechanisms in hydropower systems has become increasingly important. The dynamic nature of hydropower systems presents challenges in maintaining stable operations under varying load conditions Zhao et al. (2023).

The importance of dynamic models in hydropower systems can not be overstated. It serves as the foundation for understanding system behavior, predicting performance, and designing effective control strategies. There has been a growing interest in developing models of physical processes that closely replicate real world systems Kishor and Fraile-Ardanuy (2017). Accurate hydropower system models help to predict power generation, design control systems, and analyze stability. Mechanistic models, built upon fundamental physical

doi:10.4173/mic.2025.2.3

principles, offer a distinct advantage in simulating hypothetical systems Vytvytskyi and Lie (2018). Francis turbines, which are widely used in medium- to high-head hydropower plants, lead to complex nonlinear dynamics due to interactions between water flow, turbine components, and generator load conditions Cervantes et al. (2024). This necessitates the development of control-oriented models that can accurately represent system behavior and facilitate the design of controllers. Here, we illustrate the suitability of the model by designing a (Proportional Integral Derivative) PID controller. However, it would be possible to use more advanced methods such as robust, adaptive, nonlinear, or predictive control structures. Modeling for control in hydropower systems, particularly with Francis turbines, involves the formulation of hydraulic, mechanical, and electrical subsystems to develop a holistic representation of the plant Brekke (2001).

In some prior work, OpenModelica Fritzson et al. (2020) has been used to encode dynamic models of hydropower systems with Francis turbines (Vytvytskyi, 2019), Pandey (2023), Adhikari et al. (2024). The work of Adhikari et al. (2024) integrated a detailed loss model Zhang (2018) into an existing mechanistic model Vytvytskyi and Lie (2018) to improve turbine performance predictions. The study reported here extends the model with a rotating aggregate, and discusses control requirements and design. In a hydropower plant with Francis turbine, guide vanes play a crucial role in regulating water flow, thereby influencing power generation and system stability. An electro hydraulic actuator controls the guide vanes, enabling rapid response to load variations. The nonlinearities in the control actuator (guide vanes with pistons) are important, but are not addressed in the work here. However, important nonlinearities and losses in the turbine, friction in pipes, etc., are incorporated in the hydraulic and mechanical dynamics Shanab et al. (2020).

Several control strategies have been proposed and applied in hydropower systems, particularly for regulating turbine speed, power output, and grid frequency LU2 (2025), Ngoma et al. (2025), Hu et al. (2023). Classical controllers remain widely used due to their simplicity, ease of use, reliability, and effectiveness in handling systems with relatively predictable and linear behaviours Cominos and Munro (2002). In recent years, advanced control approaches such as robust control, adaptive control, nonlinear control, and model predictive control (MPC) have been actively explored to overcome the limitations of classical methods Pavon et al. (2024). Robust and adaptive controllers, for instance, are designed to improve disturbance rejection and maintain stability in the presence of parameter variations. Nonlinear control strategies can better capture the complex dynamics of hydropower systems, while MPC offers the ability to explicitly handle constraints and optimize performance over a prediction horizon Nagode et al. (2022).

Despite the potential benefits of advanced controllers, PID control remains the dominant choice in many operational hydropower plants due to its well-understood behaviour, ease of implementation, minimal computational requirements, and compliance with industry regulations. Consequently, while advanced techniques are valuable for specialized applications or challenging operating conditions, classical PID control serves the industry standard in many operational hydropower for majority of practical scenarios Chen (2024).

While the previous work was focused on enhancing the turbine model, this research focuses on the development of PID controllers for regulating turbine speed, power output, and frequency stability under varying load conditions. In this study, PID control is chosen for its practical relevance and ease of integration with existing systems, while still offering valuable insights into tuning methodologies and performance trade-offs for both linear and nonlinear models. The PID controller is tuned to mitigate transient oscillations and improve dynamic response in accordance to Statnett, the Norwegian Transmission System Operator (TSO) requirements Statnett (2024), and ensure reliable grid operation. By combining a mechanistic model with classical control techniques, we present a detailed discussion of model based PID tuning of a load/frequency controller from a control engineering perspective.

The paper is structured as follows: Section 2 gives a system description of the hydropower plant model and the control requirements for the linearized and nonlinear model. Section 3 provides a summary of concepts used to develop the model, including the intake, penstock, surge tank, a mechanistic model of the Francis turbine, and aggregate along with an open-loop simulation setup. Section 4 focuses on the controller design, detailing the implementation and key findings of the study. Section 5 discusses the insights gained from the research and finally, Section 6 presents the conclusions and suggests future avenues to be explored.

2 System description

2.1 Overview of the hydropower plant

The hydroelectric system under study is a high head hydroelectric plant in Sundsbarm, Norway, which features a Francis turbine. A general layout of a hydropower plant is presented in Figure 1. The plant includes key components such as the intake, penstock,

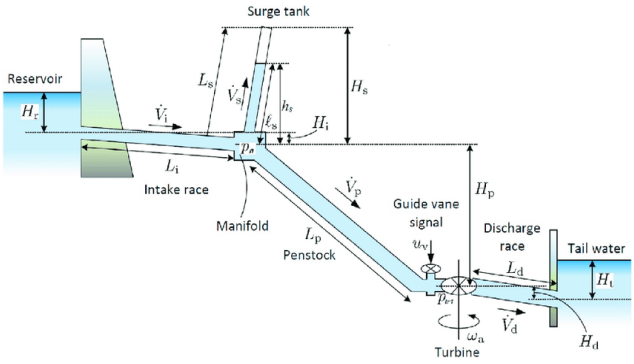

Figure 1: Geometrical layout of a hydropower plant. Adhikari et al. (2024)

surge tank, turbine, discharge race unit, and aggregate. The waterway geometry parameters are consistent with those outlined in Adhikari et al. (2024), and detailed in Table 1. The nominal variables relevant to the operation of the hydropower plant are also provided in same table. The nominal values are the operational values at Sundsbarm, using a Francis turbine and a synchronous generator. Additionally, the turbine's geometrical parameters are determined using the design algorithm described in Vytvytskyi and Lie (2018) and are summarized in Table 2. The data in Table 2 may deviate from those of the actual turbine in the Sundsbarm plant.

Table 1: System parameters including waterway geometry and nominal operational values.

Parameter	Value
Reservoir height difference [m]	48
Intake race height difference [m]	23
Intake race length [m]	6600
Intake race diameter [m]	5.8
Penstock height difference [m]	428.5
Penstock length [m]	600
Penstock diameter [m]	3
Surge tank height difference [m]	120
Surge tank length [m]	140
Surge tank diameter [m]	3.4
Discharge height difference [m]	0.5
Discharge length [m]	600
Discharge diameter [m]	5.8
Tail water height difference [m]	5
Nominal head [m]	460
Nominal discharge rate [m^3/s]	24.3
Nominal power [MW]	104.4

Table 2: Turbine/generator parameters from design procedure.

Blade inlet angle β_1[°]	Blade outlet angle β_2[°]	Inlet radius r_1[m]	Outlet radius r_2[m]	Blade width w_1[m]	Number of pole pairs
62.85	17.5	1.32	0.775	0.25	6

2.2 Control requirements

Designing an effective controller for the model requires addressing specific criteria. The following requirements are crucial for both linear and nonlinear system designs Statnett (2024).

- **Linearized model:** For the linearized model at 85% of maximal power production and 2% permanent droop the requirements are as follows:
  - Stability margins: Phase margin greater than 25 degrees, gain margin greater than 1.41 (3 dB).
  - Maximal peak in tracking from dimensionless load to dimensionless frequency is 3 dB (0 dB with a stricter standard).
  - Step response for 1% of maximal power can have maximal deviation in frequency of 1%.
- **Nonlinear model:** Similarly, for the nonlinear model, the controller needs to ensure stability during power stepping in the following settings with 2% permanent droop .
  - $\dot{W}_e$: 100% $\longrightarrow$ 85% of maximal load
  - $\dot{W}_e$: 85% $\longrightarrow$ 100% of maximal load
  - $\dot{W}_e$: 100% $\longrightarrow$ 50% of maximal load
  - $\dot{W}_e$: 100% $\longrightarrow$ 20% of maximal load

3 Model description

3.1 Hydropower model

The hydropower plant is modelled using differential algebraic equations (DAEs) model of each hydropower component. Output of the previous component act as the input for the following component. The overall hydropower model is divided into two parts: the waterway model and the aggregate model which consists of the rotational mass of the combined turbine and synchronous generator, and is finally connected to the electric grid. The waterway consists of reservoir, intake race, manifold, surge tank, penstock, discharge

race and tail race, while the electro-mechanical subsystem encapsulates the rotating mass of the turbine with guide angle actuators, and the generator.

As discussed in Adhikari et al. (2024), the dynamic model of the hydropower system is based on using (steady state) total mass balance, linear momentum balance for the water pipes, and (steady state) angular momentum balance for the turbine. Here, we extend this model by applying the rotational kinetic energy balance for the aggregate.

The waterway channel starts at the reservoir and ends at the tailrace. The complete model of the waterway unit is discussed in detail in Adhikari et al. (2024).

A Francis turbine is modelled using the angular momentum balance (Euler equations) [1], (Zhang, 2018). The model for primary losses prevalent in the turbine, i.e., friction, swirl loss and shock loss are used as in Adhikari et al. (2024).

The hydropower model discussed in Adhikari et al. (2024) does not include the aggregate model. Hence, the aggregate model is added for the control study in this paper. The aggregate comprises of the turbine and the synchronous generator. The aggregate rotation is modelled via the kinetic energy balance and expressed as:

$$\frac{dK_\mathrm{a}}{dt} = \dot{W}_\mathrm{ts} - \dot{W}_\mathrm{f,a} - \dot{W}_\mathrm{e}. \tag{1}$$

Total kinetic energy K_a is given by:

$$K_\mathrm{a} = \frac{1}{2} J_\mathrm{a} {\omega_\mathrm{a}}^2 = \frac{1}{2} J_a \left(\frac{2\pi f}{N_\mathrm{p}}\right)^2, \tag{2}$$

where,
J_a: Moment of inertia of the aggregate
ω_a: Angular velocity of the aggregate
f: System frequency
N_p: Number of pole pairs of the synchronous generator

The bearing friction dominates the total friction losses $\dot{W}_\mathrm{f,a}$ in the aggregate rotation and is expressed as:

$$\dot{W}_\mathrm{f,a} = k_\mathrm{f} {\omega_\mathrm{a}}^2, \tag{3}$$

where k_f is the friction factor in the aggregate bearing box.

The waterway model is connected to only one aggregate for the grid, limiting the study to an isolated operation.

3.2 Model validation

The hydropower model is developed using the parameters presented in Tables 1 and 2. Its validity is assessed by comparing turbine shaft power, turbine friction terms, and turbine efficiency with corresponding values from the commercial software Alab provided in Vytvytskyi and Lie (2018). In the absence of exact actual operational measurement data from the Sundsbarm plant, validation is performed through visual comparison of model outputs with the simulation results reported in Adhikari et al. (2024). While this approach provides a qualitative indication of consistency, it does not confirm quantitative agreement with real plant behaviour. Consequently, the practical applicability of the designed controller cannot be fully established without empirical validation.

3.3 Open loop simulation

An open loop simulation model of the hydropower system is presented in Figure 2. Open loop simulation represents the system's behaviour in the absence of any control mechanism. This allows for the identification of system instabilities or performance limitations, thereby demonstrating the necessity of incorporating a controller. Figure 2 presents the complete hydropower model, which includes the surge tank. But for the purpose of analysis, open loop simulations have been carried out for two configurations: with and without the surge tank.

3.3.1 Step response without controller for small load changes

An open loop simulation setup was used to evaluate the system's response to small step changes of 1% from nominal load set at 85% of maximum load. The load was initially maintained at 85% i.e, starting at steady state, then stepped up to 86%, reverted to 85%, stepped down to 84% and finally returned to 85%. The resulting responses in grid frequency is presented in Figure 3. This result demonstrates that even minor load changes may cause significant deviations in frequency. The results show that even small variations lead to frequency deviations beyond the allowable range of ± 0.5 Hz in both models, with and without the surge tank. This highlights the necessity of implementing an effective controller to maintain frequency stability and address this issue.

Likewise, with the open loop simulation for the model with and without surge tank, the pressure drop immediately upstream of the turbine is of interest to study. The result for the pressure drop is as shown in Figure 4. The results show that the surge tank serve the purpose: to reduce the water hammer, and thus the mechanical tear of the guide vanes/turbine.

[1] From unpublished notes by B. Lie (2023).

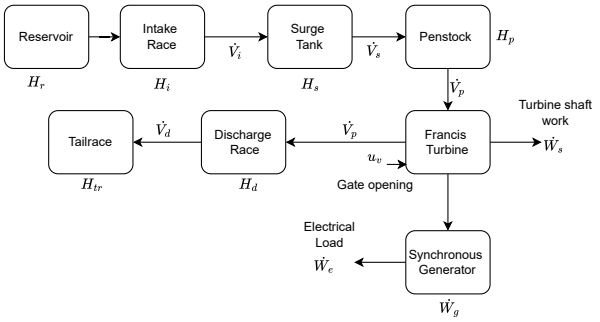

Figure 2: Open loop simulation model.

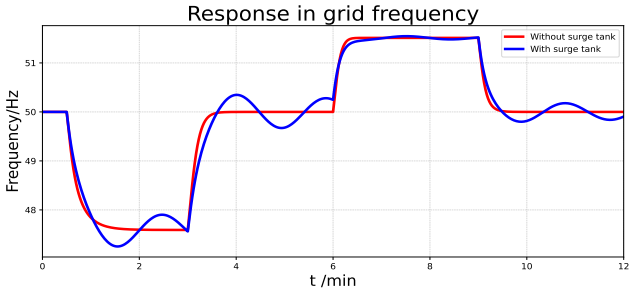

Figure 3: Response in grid frequency upon 1% step change in power load from nominal load.

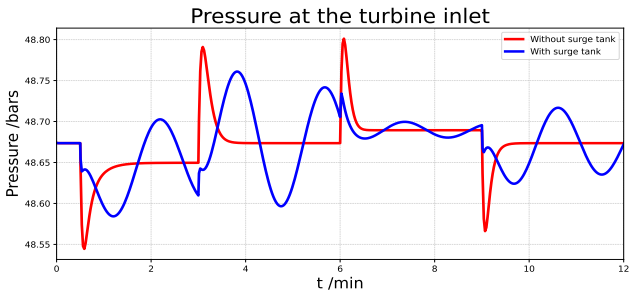

Figure 4: Turbine inlet pressure drop upon 1% step change in power load from nominal load.

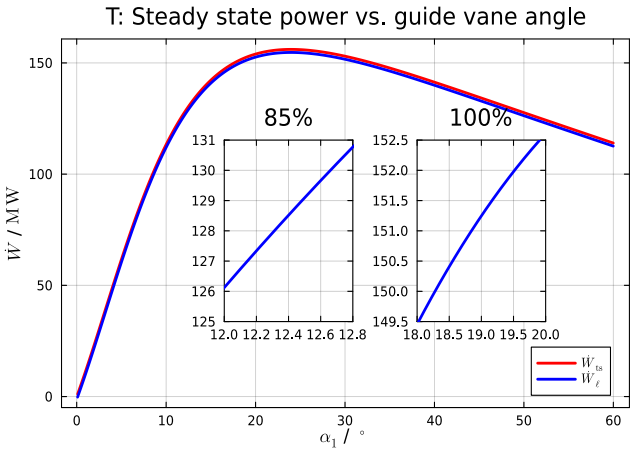

Figure 5: Turbine shaft power and corresponding load, as a function of guide vane angle in steady state.

4 Controller design and testing

Before moving into the controller design, some steady state tests are done. The case without a surge tank is explored for simplicity. With the given design of the turbine, the turbine shaft power $\dot{W}_{\mathrm{ts}}$ in steady state is given as a function of the guide vane angle α_1, as illustrated in Figure 5.

The system gain is the gradient of the power with respect to guide vane angle as indicated in Figure 5. It is clearly seen that the system transitions from a positive gain to a negative gain at approximately angle $\alpha_1 = 23.8°$. For guide vane angles above $\alpha_1 = 60°$, the dynamic system becomes unstable, and no steady state exists. The change in the sign of the gain is a result of increased losses (friction, shock, swirl) in the turbine. Stretching the operating regime across a change in gain would make controller design difficult. Some industrial high-pressure Francis turbines are known to limit the guide vane angle to 18°–20°.

To avoid the negative gain and extreme nonlinearity indicated in Figure 5, the maximal allowed guide vane angle is (somewhat arbitrarily) set to $\alpha_{1,\max} = 18.2°$, corresponding to a load $\dot{W}_{\mathrm{l,max}} \approx 150\,\mathrm{MW}$. The corresponding guide vane angle for $0.85\,\dot{W}_{\mathrm{l,max}} \approx 127.5\,\mathrm{MW}$ is $\alpha_{1,85\%} \approx 12.2°$.

In any hydropower operation, maintaining the grid frequency at or near a specified reference value typically – 50 Hz in regions such as Asia and Europe – is essential for stable power system performance. In the case of isolated operation, where a single turbine-generator unit supplies power to the grid, frequency regulation if often achieved using a PID controller.

4.1 Control for model linearized at 85% of maximal load

The model is linearized around 85% of the maximal load. Model linearization was done using the Julia packages: ModelingToolkit.jl Ma et al. (2021) and ControlSystems.jl Bagge Carlson et al. (2021). The plant model, $P_{\mathrm{a,u_v2f}}(s)$ is the transfer function that characterizes the relationship between the guide vane signal, u_{v} and the system frequency, f. Subscript "a" indicates the model pertaining the dynamics of the system from the reservoir to "a" for aggregate. The transfer function $P_{\mathrm{a,u_v2f}}(s)$ is as follows (transfer function from the actuator is not included):

$$P_{a,u_v2f}(s) = 129 \cdot \frac{1 - 2.66s}{(1 + 3.08)(1 + 6.44s)} \tag{4}$$

Similarly, $P_{\mathrm{a,\dot{W}_e2f}}(s)$ is the transfer function from disturbance, $\dot{W}_e$ to system frequency, f and is as follows:

$$P_{\mathrm{a,\dot{W}_e2f}}(s) = 1.18 \cdot 10^{-6} \cdot \frac{1 + 1.53s}{(1 + 3.08)(1 + 6.44s)} \tag{5}$$

From the transfer function in Eq. 4, a simple PID is designed to cancel the slowest time constant (6.44) with the integral time T_{i}, and the fastest time constant (3.08) with the derivative time T_{d}.

Observe that using a tuning rule such as Skogestad's rule Skogestad (2004) with modification to handle the right half plane zero (at 2.66) here will give the same values for T_{i} and T_{d}. Skogestad's method will also give a value for K_{p} that ensures good stability margin, but gives "too good" margin for our case.

The PID controller $C_{\mathrm{pid}}(s)$ thus becomes

$$C_{\mathrm{pid}}(s) = K_{\mathrm{p,pid}} \cdot \frac{1 + 6.44s}{6.44s} \cdot \frac{1 + 3.08s}{1 + 0.1 \cdot 3.08s} \tag{6}$$

Filter time constant for the derivative action is set to $\tau_f = 0.1T_d$.

The loop transfer function $L_{\mathrm{pid}}(s)$ is

$$L_{\mathrm{pid}}(s) = P_{\mathrm{a,u_v2f}}(s) \cdot C_{\mathrm{pid}}(s) \tag{7}$$

Initially, we set $K_{\mathrm{p,pid}}$ to unity, and then K_{p} is chosen to get adequate stability margin to fulfil the requirements in Section 2. After appropriate tuning, the stability margins are obtained as shown in Figure 6.

From Figure 6 we see that gain margin is barely sufficient, while the phase margin is better than required as mentioned in Statnett (2024).

Similarly, the resulting (dimensionless) transfer function from load $\dot{W}_{\mathrm{e}}$ to frequency f_{e} is given in Figure 7.

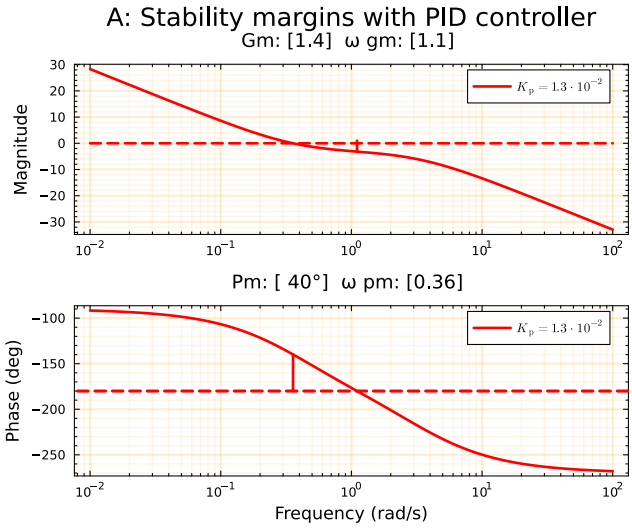

Figure 6: Stability margins for PID controller.

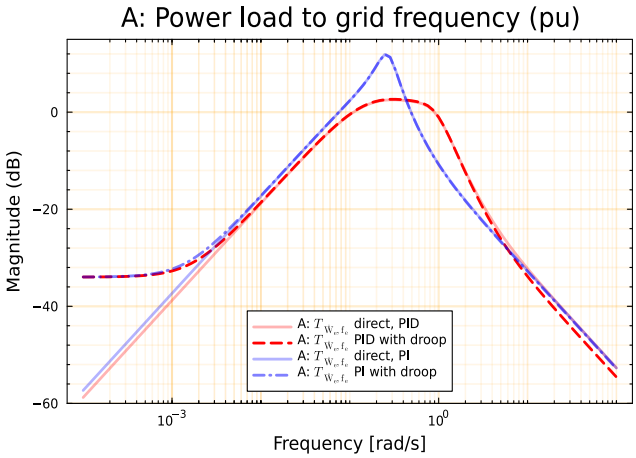

Figure 7: Tracking from $\dot{W}_e$.

From Figure 7 it is not possible to tune the gain in the PI controller to achieve maximal peak in tracking to $\leq$ 3dB. Figure 7 illustrates that we can almost satisfy the requirements of disturbance attenuation if we use a PID controller. More generally, we have an optimization problem where we need to balance the stability margins against disturbance attenuation. We could have achieved a better result by formalizing this balancing as an optimization problem, and then modified all three controller parameters T_{i}, T_{d}, and K_{p}. Such an optimization is not considered here, though.

To evaluate the third requirement, maximum 1% deviation in frequency to a 1% change in load, closed loop 1% step response from load $\dot{W}_e$ to grid frequency f_e is plotted and presented in Figure 8, using the linearized model.

Figure 8 indicates that the PID controller does not

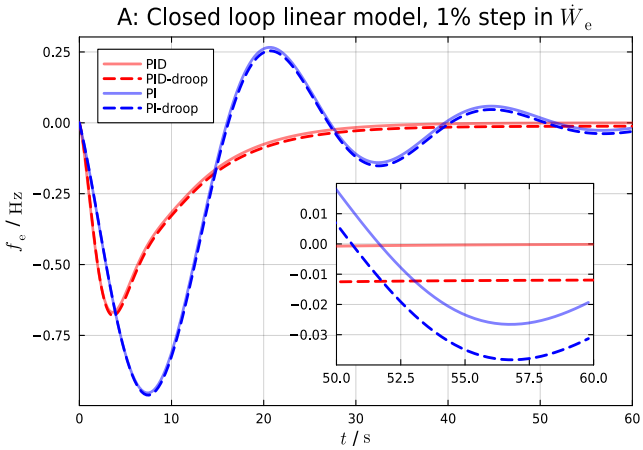

Figure 8: Closed loop step response from load to grid frequency based on the linear model with controller.

satisfy the maximally allowed deviation in frequency. The frequency deviation is close to 1.4%, while the requirement is not more than 1% . In Figure 8, we have included permanent droop in the controller. The permanent droop is a method to spread an unexpected load in the system on several aggregates. Figure 8 indicates that a permanent droop gives a small stationary deviation in grid frequency after a step change in the load: observe the red, dashed line in Figure 8 that has a steady state different from 0. Since this study involves an isolated system with a single aggregate serving a single load, droop serves no purpose, and is not used in the rest of the study.

4.2 Control of nonlinear system

After completing the control design for the linearized system, the focus shifts to testing the developed controller on the nonlinear system. In doing so, some changes to controller parameters should be expected, see the nonlinear gain in the system as indicated by Figure 5. Whereas closed loop performance can be assessed analytically for the linear model, this is difficult for the nonlinear model, and therefore the analysis of the PID controller applied to the nonlinear model is given via simulations, which is in accordance with the TSO requirements from Statnett (2024). For the nonlinear model, the initial value of PID controller gain, $K_{\text{pid}} = 1.3 \cdot 10^{-3}$, concluded to be too large for achieving good performance. To enhance the closed loop response and overall system performance, the PID gain used for the linear approximation was divided by a factor of 2.8. This adjustment is necessary to account for the nonlinearity in the system, ensuring improved stability and better adherence to the desired control objectives.

4.2.1 Small power load changes

Firstly, small load changes are made for the nonlinear model with the controller. From the baseline of 85% of the maximum power load in the steady state operation, the load is increased to 86%, then returned to 85% then lowered to 84% and finally returned to the initial case, i.e., 85%. The results for respective frequency deviations and guide vane signal are shown in Figures 9 and 10, respectively.

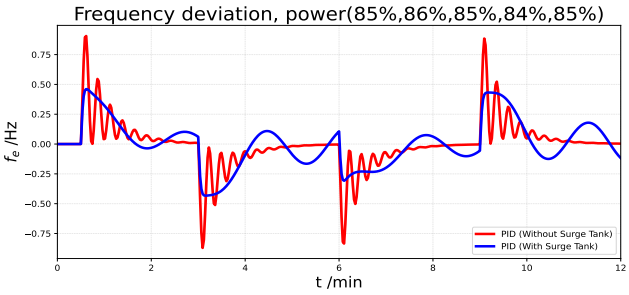

Figure 9: Response in grid frequency deviation to small changes in power load.

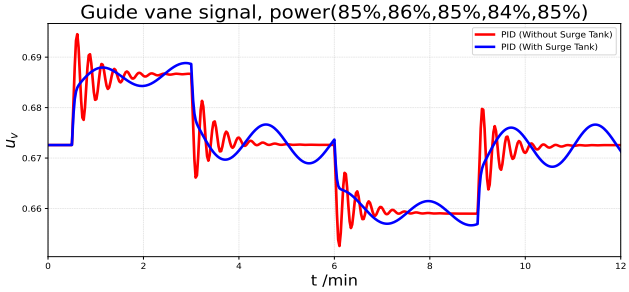

Figure 10: Response in guide vane signal to small changes in power load.

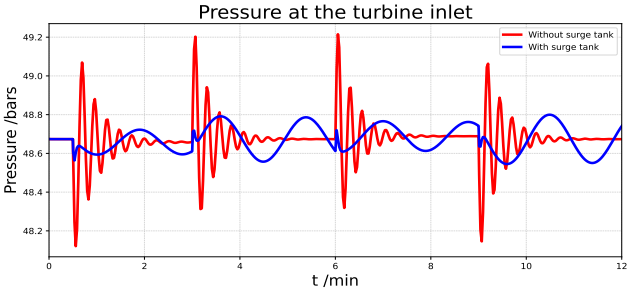

Figure 11: Turbine inlet pressure drop for small load changes.

Figure 9 shows that the controlled frequency deviation is within the allowable range of ±1% (±0.5 Hz) for the model with surge tank. We also observe from Figure 10 that the control signal, u_v is well within the range [0,1] for both cases.

Figure 11 illustrates the pressure at the turbine inlet for the model with the controller under small load variations. As the controller actively regulates system frequency, it continuously adjusts the guide vane signal. This dynamic control action helps to stabilize the pressure fluctuations at the turbine inlet, ensuring smoother system operation.

4.2.2 Large power load changes

After the controller is tested with small load changes, the next step is to check for the larger load changes according to the requirements in Section 2.2. Starting at steady state condition based on the baseline of 85% of the maximal power load, the load is increased to 92%, then returned to 85%, lowered to 50%, then finally lowered to 20%. The results for the frequency deviation and guide vane signal is shown in Figures 12 and 13, respectively.

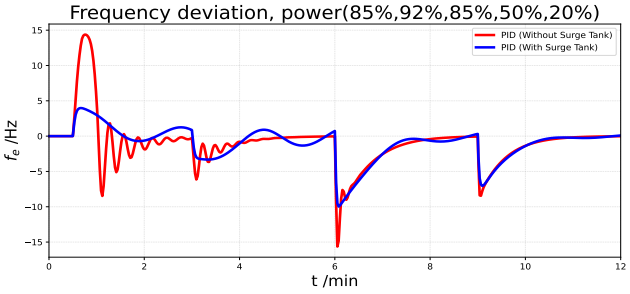

Figure 12: Response in grid frequency deviation to large changes in power load.

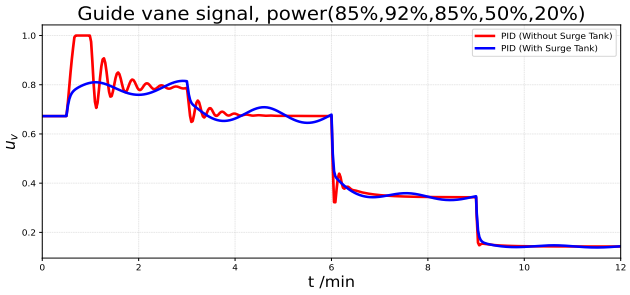

Figure 13: Response in guide vane signal to large changes in power load.

Such large power load variations give a large frequency deviation. According to the control requirements for the nonlinear model as detailed in Section 2.2, we should test the controller by stepping up to 100% of the power load, and then down to 20%. However, the system becomes unstable if we step the load to a higher value than 92% for the model without surge tank and 94.4% for the model with surge tank. In this regard, the test fails. This is partially due to the nonlinearity in the system at $\alpha_{1,\max} = 18.2$ degrees, and uncertainty in how to choose the maximally allowed power. But the interesting fact is that the frequency deviation for the model with surge tank is significantly less than compared to the model without surge tank.

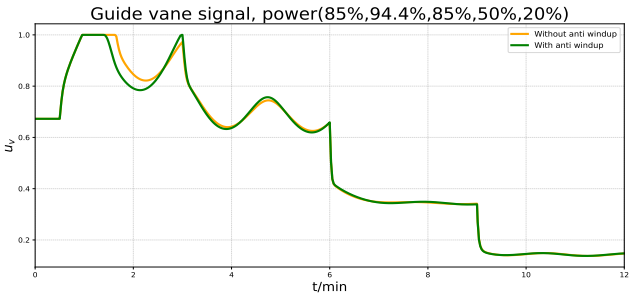

Figure 14: Response in guide vane signal to large changes in power load with and without anti-windup action.

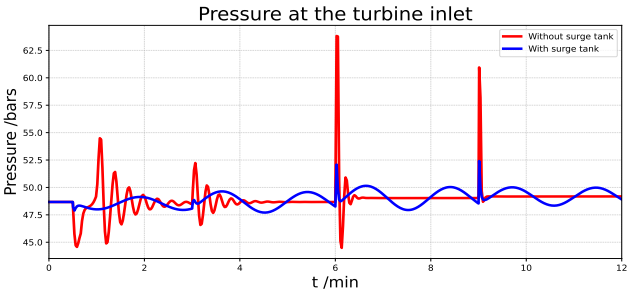

Figure 15: Turbine inlet pressure drop for large load changes.

As shown in Figure 13, the guide vane signal u_v experiences clipping for approximately 20 seconds during stepping up the power load to 92% of the maximally allowed power load for the model without the surge tank. In contrast, the model with a surge tank can handle a higher power load stepping up to 94.4%. In this case, the guide vane signal clips at its upper limit of 1, as illustrated in Figure 14. To address this clipping, an anti-windup action is implemented, the clipping duration of the guide vane signal is considerably reduced, on doing so also demonstrated in Figure14.

Figure 15 depicts the pressure at the turbine inlet during large load variations. In the absence of a surge tank, the controller's effort to regulate frequency leads to significant pressure oscillations, resulting in a

pronounced water hammer effect. However, when the surge tank is included, this effectively dampens these oscillations and mitigates the water hammer, highlighting its crucial role in stabilizing hydraulic transients during sudden operational changes.

5 Discussion

This study provides insights into control relevant models and controller design for hydropower systems. Beginning with open-loop operation to motivate for the need for a controller, a linear PID controller with actuator saturation was tested both on a linear model and on the full nonlinear hydropower model by analysis and simulation. The control strategy was explored through closed-loop simulations under varying load conditions ranging from small to large disturbances. Recognizing the need for a controller to handle some model uncertainty and load variations, a controller was designed in reference to the Statnett standards in Section 2.2.

Initially, the controller was developed for a linearized system without a surge tank. This simplification allowed for a more straightforward control design, serving as a foundation for further development. The surge tank known for its critical role in dampening pressure oscillations and mitigating transients during sudden turbine operation changes was then integrated into the nonlinear model to study its stabilizing effect.

Subsequently, the same control designs were tested on the nonlinear system both with and without the surge tank. The results revealed that, in both cases, the PID controller gains needed to be reduced by approximately a factor of 2.8 to achieve better performance. This adjustment underscores the importance of system nonlinearity in tuning control parameters for stable and efficient hydropower operation.

The controller design could also have been enhanced by optimizing parameters simultaneously to achieve stability margins and disturbance suppression. In the current simplified approach, the design prioritizes stability margins, which meets foundational requirements but does not fully capitalize on the potential for improved disturbance handling. A dual-objective optimization strategy could provide better results, especially in reducing the maximum gain from disturbances to frequency.

Another key consideration is the choice of maximum guide vane angle, $\alpha_{1,\max}$. This parameter was set at 18.2°, based on industry reports of maximum 18-20 degrees, in combination with reducing the nonlinearity as much as possible. $\alpha_{1,\max} = 14$ degrees, the nonlinearity would have been much smaller. On the other hand, exceeding 23.5° leads to a negative system gain, which complicates control and should be avoided. Despite this, the selection of $\alpha_{1,\max}$ remains questionable, as it does not account for factors such as the nominal power or the generator's thermal limits. Lowering $\alpha_{1,\max}$ would simplify control by reducing the system nonlinearity, though it would also limit power output. Alternative turbine parameter design algorithms, such as those proposed by Zhang (2022), could alter the steady state relationship between α_1 and power production, significantly impacting system behaviour.

All the simulations in this study are with fixed reservoir height. It would also be of interest to observe how much a change in reservoir height influences the system.

Finally, the assumption that the load on the generator terminals is a true load simplifies the analysis but may not reflect real-world dynamics. A more realistic approach would involve modelling the generator with field voltage control and an infinite bus Nielsen (1996). This inclusion would provide a more accurate representation of system behaviour and facilitate more robust controller design.

6 Conclusion

This study highlights several key insights into the design of controllers for hydropower systems. The work presented a systematic approach to PID controller design for an isolated hydropower system equipped with a Francis turbine, using a mechanistic model formulated in differential algebraic equations. The critical role of surge tanks and the interplay between stability margins and disturbance suppression have been explored, underscoring the trade-offs inherent in controller design. The gain adjustment necessity when shifting from linear to nonlinear operation highlighted the need to account for hydraulic dynamics and nonlinearities in controller tuning. The current approach prioritizes stability, yet results suggest that incorporating a dual-objective optimization could further enhance performance. Additionally, the selection of maximum guide vane angle, $\alpha_{1,\max}$ was shown to have a significant impact on control complexity and system nonlinearity, with lower values simplifying control at the expense of maximum power output, leaving room for improvement in its determination.

Future work should explore alternative turbine parameter design algorithms, such as those proposed by Zhang (2022), to enhance system performance. Incorporating more realistic consumer load profiles could provide a closer approximation of real-world conditions, thereby improving the applicability of the results. Additionally, advanced controller designs that balance stability margin optimization and disturbance suppression merit further investigation. Finally, in-

tegrating generator dynamics, including field voltage control and an infinite bus, would offer a more holistic understanding of the system, enabling more refined and effective control strategies.

Acknowledgments

The first author gratefully acknowledges the support of the Norwegian Program for Capacity Development in Higher Education and Research for Development (NORHED) for the Research Based Education for Development of Hydropower Professionals for the Himalayan Region (Hydro-Himalaya) project. The third author acknowledges discussions with Dr. Bjarne Børresen in Multiconsult Norge AS. Any misunderstandings from those discussions are due to the third author, and not Dr. Børresen.

References

Primary frequency regulation performance in hydropower systems: Precise quantification and holistic enhancement under wide-range operation. *Applied Energy*, 2025. 389:125711. doi:10.1016/j.apenergy.2025.125711.

Adhikari, U., Shrestha, P., and Lie, B. Hydropower system with francis turbine for control-study. In *2024 IEEE International Conference on Power System Technology (PowerCon)*. pages 1–5, 2024. doi:10.1109/PowerCon60995.2024.10870523.

Bagge Carlson, F., Fält, M., Heimerson, A., and Troeng, O. ControlSystems.jl: A Control Toolbox in Julia. In *2021 60th IEEE Conference on Decision and Control (CDC)*. pages 4847–4853, 2021. doi:10.1109/CDC45484.2021.9683403.

Brekke, H. *Hydraulic Turbines: Design, Erection and Operation*. Norwegian University of Science and Technology (NTNU), Trondheim, Norway, 2001. URL https://www.ntnu.no/documents/381182060/1267681377/HYDRAULIC+TURBINES_Hermod+Brekke+-+2015.pdf.

Cervantes, M. J., Sundström, J., Shiraghaee, S., Kjeldsen, M., and Wiborg, E. J. Extending the operational range of francis turbines: A case study of a 200 mw prototype. *Energy Conversion and Management: X*, 2024. 23:100681. doi:10.1016/j.ecmx.2024.100681.

Chen, R. A comprehensive analysis of pid control applications in automation systems: Current trends and future directions. In *Highlights in Science, Engineering and Technology, Vol. 97 (2024): Proceedings of the 7th International Conference on Mechatronics, Control and Electronic Engineering (MCEE 2024)*. Darcy & Roy Press Co., pages 126–132, 2024. doi:10.54097/6q4xxg69.

Cominos, P. and Munro, N. Pid controllers: Recent tuning methods and design to specification. *Control Theory and Applications, IEE Proceedings* -, 2002. 149:46 – 53. doi:10.1049/ip-cta:20020103.

Fritzson, P., Pop, A., Abdelhak, K., Asghar, A., Bachmann, B., Braun, W., Bouskela, D., Braun, R., Rogovchenko-Buffoni, L., Casella, F., Castro, R., Franke, R., Fritzson, D., Gebremedhin, M., Heuermann, A., Lie, B., Mengist, A., Mikelsons, L., Moudgalya, K., and Östlund, P. The openmodelica integrated environment for modeling, simulation, and model-based development. *Modeling, Identification and Control: A Norwegian Research Bulletin*, 2020. 41:241–295. doi:10.4173/mic.2020.4.1.

Gunatilake, H., Wijayatunga, P., and Roland-Holst, D. Hydropower Development and Economic Growth in Nepal. 2020. doi:10.22617/WPS200161-2.

Hu, X., Wang, T., Chen, K., and Ye, P. Research on control system for improving the grid-connected efficiency of small hydropower. *Energy Reports*, 2023. 9(24):772–783. doi:10.1016/j.egyr.2023.04.344.

Kishor, N. and Fraile-Ardanuy, J. *Modeling and Dynamic Behaviour of Hydropower Plants*. 2017. doi:10.1049/PBPO100E.

Ma, Y., Gowda, S., Anantharaman, R., Laughman, C., Shah, V., and Rackauckas, C. Modelingtoolkit: A composable graph transformation system for equation-based modeling. 2021. doi:10.48550/arXiv.2103.05244.

Nagode, K., Škrjanc, I., and Murovec, B. Enhanced stability and failure avoidance of hydropower plant in contingent island operation by model predictive frequency control. *Energy Reports*, 2022. 8:9308–9330. doi:10.1016/j.egyr.2022.07.040.

Ngoma, D. H., Mfangavo, A., and Masenga, B. Comparative control governor systems for power and frequency optimization of an islanding off-grid small hydropower plant. *Discover Energy*, 2025. 5(6). doi:10.1007/s43937-025-00066-8.

Nielsen, T. K. Dynamic Behaviour of Governing Turbines Sharing the Same Electrical Grid. In E. Cabrera, V. Espert, and F. Martínez, editors, *Hydraulic Machinery and Cavitation*, pages 769–778. Springer

Netherlands, Dordrecht, 1996. doi:10.1007/978-94-010-9385-9_78.

Pandey, M. *Modelling Tool for Hydropower Systems, with Analysis and Design*. Ph.D. thesis, University of South-Eastern Norway, 2023. URL https://openarchive.usn.no/usn-xmlui/handle/11250/3093026. Accepted: 2023-09-29T09:52:03Z ISSN: 2535-5252.

Pavon, W., Jaramillo, M., and Vasquez, J. C. A review of modern computational techniques and their role in power system stability and control. *Energies*, 2024. 17(1):177. doi:10.3390/en17010177.

Shanab, B. H., Elrefaie, M. E., and El-Badawy, A. A. Active control of variable geometry francis turbine. *Renewable Energy*, 2020. 145:1080–1090. doi:10.1016/j.renene.2019.05.125.

Skogestad, S. Process control: Lecture notes. https://techteach.no/presentations/tekna_olje_gass_04/lecture/documents/skogestad.pdf, 2004.

Statnett. NVF 2024 Nasjonal veileder for funksjonskrav i kraftsystemet. Technical Report 2023/3883-28, Statnett, 2024. URL https://www.statnett.no/globalassets/for-aktorer-i-kraftsystemet/systemansvaret/retningslinjer-fos/nvf-2024---nasjonal-veileder-for-.funksjonskrav-i-kraftsystemet.pdf.

Vinod, J., Sarkar, B. K., and Sanyal, D. Flow control in a small francis turbine by system identification and fuzzy adaptation of pid and deadband controllers. *Renewable Energy*, 2022. 201:87–99. doi:10.1016/j.renene.2022.11.039.

Vytvytskyi, L. *Dynamics and model analysis of hydropower systems*. Doctoral thesis, University of South-Eastern Norway, 2019. URL https://openarchive.usn.no/usn-xmlui/handle/11250/2608105. Accepted: 2019-08-13T11:10:38Z ISSN: 2535-5252.

Vytvytskyi, L. and Lie, B. Mechanistic model for francis turbines in openmodelica. *IFAC-PapersOnLine*, 2018. 51(2):103–108. doi:10.1016/j.ifacol.2018.03.018.

Zhang, Z. Master equation and runaway speed of the Francis turbine. *Journal of Hydrodynamics*, 2018. 30(2):203–217. doi:10.1007/s42241-018-0026-5.

Zhang, Z. Improvement and extension of cordier diagram for hydraulic turbines. *Proceedings of the Institution of Mechanical Engineers, Part A: Journal of Power and Energy*, 2022. 236(7):1309–1319. doi:10.1177/09576509221092282.

Zhao, Z., Ding, X., Behrens, P., Li, J., He, M., Gao, Y., Liu, G., Xu, B., and Chen, D. The importance of flexible hydropower in providing electricity stability during china's coal phase-out. *Applied Energy*, 2023. 336:120684. doi:10.1016/j.apenergy.2023.120684.